

# SCIENTIFIC REPORTS



OPEN

## Diabetes Mellitus is Associated with More Severe Brain Spontaneous Activity Impairment and Gray Matter Loss in Patients with Cirrhosis

Yun Fei Wang, Xiang Kong, Guang Ming Lu & Long Jiang Zhang

Recent studies showed many cirrhosis patients may have diabetes mellitus (DM), however, the effect of DM on brain in cirrhotic patients is unclear. This study included 34 cirrhosis patients (17 with DM, 17 without DM) and 17 age-, sex-matched healthy controls. MRI examination and neuropsychological tests were performed. Fractional amplitude of low-frequency fluctuation (fALFF) and voxel-based morphometry algorithms were used to obtain fALFF values and gray matter volume, which were compared and correlated with clinical variables. In cirrhosis patients with and without DM, fALFF values were decreased in the left postcentral gyrus, right precentral gyrus, left supramarginal gyrus, bilateral lingual gyri and occipital lobe, while increased in the left orbital frontal gyrus. Gray matter volume was decreased in bilateral caudates and putamen, while increased in bilateral thalami. Compared with non-DM cirrhosis patients, DM cirrhosis patients showed decreased fALFF values in bilateral caudates and decreased gray matter volume in bilateral thalami. The blood glucose levels of cirrhosis patients showed negative correlations with fALFF values in bilateral caudates and gray matter volume in bilateral thalami. In conclusion, DM aggravates brain damage in cirrhotic patients. Thus, it is important to pay more attention to the management of DM in cirrhotic patients.

Liver cirrhosis is a common metabolic disease which leads to multi-system lesions. Brain is one of the affected organs. Numerous studies have reported the adverse effects of liver cirrhosis on structural and functional brain reorganization, thus leading to cognitive dysfunction in these patients<sup>1-4</sup>. Moreover, Garcia *et al.* reported that up to 96% of patients with cirrhosis may be glucose intolerant and 30% patients may have type 2 diabetes mellitus (T2DM)<sup>5</sup>. Another study has demonstrated that coexistent diabetes exacerbates progression of hepatic fibrosis<sup>6</sup>. Recently, a meta-analysis study concluded that T2DM was associated with relative 1.5-fold increased risk for clinically defined Alzheimer disease and 2.5 for vascular dementia compared to non-diabetic individuals<sup>7</sup>. Furthermore, one recent prospective study showed that elevated blood glucose in the absence of DM increased the risk of dementia<sup>8</sup>. Given the high prevalence of DM in the liver cirrhosis population, a better understanding of the impact of DM offers significant opportunities to improve patient's outcome.

Multimodality MR imaging has been the most important neuroimaging tool to detect the structural and functional changes of human brain in various metabolic brain diseases<sup>9</sup>. For example, voxel-based morphometry (VBM) algorithm is a useful method for evaluating cerebral structural changes in various neurodegenerative diseases<sup>10</sup>, which allows an unbiased search of structural abnormalities across the whole brain<sup>11</sup>. Previous VBM studies showed that loss of brain tissue volume is common in DM and liver cirrhosis<sup>12, 13</sup>. On the other side, resting-state functional MRI (rs-fMRI) allows measuring the spontaneous fluctuations of blood oxygenation level-dependent signal, describing the temporal correlation of neuronal activity across distinct regions<sup>14</sup>. Fractional amplitude of low-frequency fluctuation (fALFF) algorithm is a commonly used method which can provide the information regarding the differences in baseline brain activity involved in physiological and

Department of Medical Imaging, Jinling Hospital, Medical School of Nanjing University, Nanjing, 210002, China. Correspondence and requests for materials should be addressed to L.Z. (email: [kevinzhj@163.com](mailto:kevinzhj@163.com))

Variables	Diabetic cirrhosis (n = 17)	Non-diabetic cirrhosis (n = 17)	Healthy controls (n = 17)	P value
Age (y)	54.8 ± 8.3	53.4 ± 5.9	54.4 ± 7.9	0.842 <sup>a</sup>
Gender (M/F)	12/5	12/5	12/5	0.999 <sup>b</sup>
NCT-A (s)	52.8 ± 20.0	48.1 ± 12.8	36.8 ± 9.1	0.018 <sup>c</sup>
DST (n)	34.5 ± 10.9	40.5 ± 12.5	52.4 ± 8.9	0.001 <sup>a</sup>
Child-Pugh scale (A/B/C)	15/1/1	15/1/1	none	0.999 <sup>c</sup>
HE (N/M/S)	15/1/1	15/1/1	none	0.999 <sup>c</sup>
Ascites (N/M/S)	9/5/3	11/6/0	none	0.193 <sup>c</sup>
TB (μ mol/L)	26.9 (36.2–15.8)	28.2 (38–17.1)	none	0.692 <sup>c</sup>
Albumin (g/L)	35.8 ± 6.5	35.1 ± 6.0	none	0.804 <sup>d</sup>
PT (s)	14.1 (15.5–13.1)	16.2 ± 3.0	none	0.063 <sup>c</sup>
Ammonia (μ mol/L)	54.5 ± 24.7	39 (76.5–11.5)	none	0.480 <sup>c</sup>
ALT (U/L)	39.6 ± 27.9	31 (39–22)	none	0.823 <sup>c</sup>
AST (U/L)	41.6 ± 21.3	39 (55–27.5)	none	0.796 <sup>c</sup>
Glucose (mmol/L)	7.3 ± 1.3	4.6 (5.1–4.2)	none	0.001 <sup>c</sup>
Cirrhosis duration (y)	3.2 ± 2.9	2.4 ± 2.5	none	0.380 <sup>d</sup>

**Table 1.** Demographic, clinical and neuropsychological data of the three groups Mean ± standard deviation; Median and inter-quartile range [M (QU-QL)]. P values indicate significant differences across groups. <sup>a</sup>analysis of variance; <sup>b</sup>chi square test; <sup>c</sup>k-independent samples nonparametric tests <sup>d</sup>two-sample t tests. y = year; M = male; F = female; NCT-A = number connection test type A; DST = digit symbol test; s = second; n = number; HE = hepatic encephalopathy; N = none; M = mild; S = severe; TB = total bilirubin; PT = prothrombin time; ALT = alanine transaminase; AST = aspartate transaminase.

pathological states<sup>15</sup>. It has been demonstrated that brain resting state functional connectivity coupled with structural connectivity<sup>16</sup>. This coupling was disrupted in various brain diseases<sup>17–20</sup>.

Because both brain atrophy and cognitive impairments occur in patients with cirrhosis and DM, thus, in the current study, we have a hypothesis that the presence of T2MD may increase the risk of complication in the brain of cirrhosis patients who may suffer from much more severe brain structural and functional abnormality. To our knowledge, no neuroimaging studies have been published to study the effects of DM on brain structural and functional reorganization in the patients with liver cirrhosis. In this study, we combined VBM and fALFF algorithms to simultaneously quantify gray matter volume and spontaneous brain activity damage to define the effect of DM on brain structural and functional changes in cirrhosis patients.

## Results

**Demographics, Clinical and Neuropsychological Data.** Demographic, clinical and neuropsychological data of the three groups are listed in Table 1. The differences were not found for age or gender among the three groups (both  $P > 0.05$ ). Both patient groups had a poorer performance for NCT-A and DST than the controls (both  $P < 0.05$ ). However, for the comparison between the patient groups, diabetic cirrhosis patients showed the worse performance in the neuropsychological tests than non-diabetic cirrhosis patients (both  $P < 0.05$ ).

**Regional gray matter volume differences of the three groups.** Compared with healthy controls, diabetic cirrhosis patients exhibited diffuse bilaterally symmetrical decreased gray matter (labeled in cold color) volume in the bilateral caudates, putamen and lingual gyri and increased volume (labeled in warm color) in bilateral thalami. Non-diabetic cirrhosis patients exhibited similar gray matter volume changes (Table 2). In the comparison between the two patient groups, diabetic cirrhosis patients presented bilaterally decreased gray matter volume of thalamus compared with non-diabetic cirrhosis patients (Fig. 1, Table 2).

**fALFF differences of the three groups.** Compared to controls, patients with liver cirrhosis showed widespread fALFF differences ( $P < 0.05$ , Alphasim corrected, cluster size  $> 98$ ). These two patients groups showed both decreased fALFF value (labeled in cold color) in both cortical and subcortical regions (including the left postcentral gyrus, right precentral gyrus, left supramarginal gyrus, occipital lobe, and bilateral lingual gyri) and increased fALFF value (labeled in warm color) in the left frontal lobe. In the comparison between the patient groups, diabetic cirrhosis patients presented decreased fALFF signals in the bilateral caudates compared with non-diabetic cirrhosis patients (Fig. 2, Table 3).

**Correlation analysis results.** There was a negative correlation between the blood glucose levels and the fALFF values in the bilateral caudates in all cirrhosis patients ( $r = -0.363$ ,  $P = 0.034$ ) (Fig. 3). The cirrhosis patients group also had a negative correlation between the blood glucose levels and the volume of the bilateral thalami ( $r = -0.602$ ,  $P = 0.001$ ) (Fig. 3). However, when correlating the blood glucose levels within each patient group, only bilateral thalamus volume showed negative correlation in diabetic cirrhosis patients group ( $r = -0.484$ ,  $P = 0.049$ ) and non-diabetic cirrhosis patients group ( $r = -0.569$ ,  $P = 0.017$ ) (Fig. 4). No relationships were identified in the cirrhosis patients

Anatomic Regions	Diabetic cirrhosis vs healthy controls	Non-diabetic cirrhosis vs healthy controls	Diabetic vs Non-diabetic
	MNI Coordinates (x, y, z)/t Value	MNI Coordinates (x, y, z)/t Value	MNI Coordinates (x, y, z)/t Value
Cingulum_Mid	—	(-4,-28,46)/3.72	—
Cuneus	—	(-5,-65,24)/4.56	—
Calcarines	—	(-3,-65,12)/4.01	—
Caudate_L	(-5,16,2)/-3.92	(-7,11,2)/-3.21	—
Caudate_R	(8,16,-2)/-3.35	(13,16,-4)/-3.28	—
Thalamus_L	(-6,-19,13)/3.95	(-11,-28,10)/5.29	(-6,-15,2)/-2.73
Thalamus_R	(8,-16,18)/4.93	(11,-22,10)/5.29	(7,-14,12)/-2.87
Putamen_L	(-18,6,-7)/-5.04	(-19,8,-9)/-5.29	—
Putamen_R	(19,12,-7)/-4.74	(18,12,-9)/-5.04	—
Lingual_L	(-6,-64,4)/3.65	—	—
Lingual_R	(6,-62,4)/3.89	—	—

**Table 2.** Differences of VBM among three groups. All  $P < 0.05$ , with Alphasim corrected. MNI = Montreal Neurological Institute; Mid = middle; L = left; R = right.

Anatomic Regions	Diabetic cirrhosis vs healthy controls	Non-diabetic cirrhosis vs healthy controls	Diabetic vs Non-diabetic
	MNI Coordinates (x, y, z)/t Value	MNI Coordinates (x, y, z)/t Value	MNI Coordinates (x, y, z)/t Value
Postcentral_L	(-46,-23,44)/-3.98	(-48,-23,43)/-3.77	—
Precentral_R	(48,-12,48)/-3.65	(38,-14,55)/-3.62	—
SupraMarginal_L	(-54,-21,36)/-4.34	(-53,-20,36)/-3.61	—
Cuneus	(2,-87,22)/-3.72	—	—
Calcarines	(1,-89,-2)/-3.61	—	—
Caudate_L	—	(-10,12,0)/3.12	(-9,9,0)/-3.81
Caudate_R	—	(12,12,-9)/3.50	(8,12,2)/-3.48
Occipital_Mid_L	(-23,-95,-2)/-4.27	(-40,-73,2)/-3.80	—
Occipital_Mid_R	(43,-82,4)/-3.48	(41,-82,5)/-2.97	—
Occipital_Inf_L	(-27,-95,-7)/-3.90	(-24,-93,4)/-2.88	—
Occipital_Inf_R	(30,-9,-12)/-4.25	(26,-96,-10)/-3.68	—
Lingual_L	(-29,-92,-12)/-4.14	(-32,-91,-14)/-3.52	—
Lingual_R	(28,-94,-14)/-3.97	(24,-96,-12)/-3.82	—
Frontal_Sup_Orb_L	(-12,18,-21)/3.92	(-16,20,-18)/2.96	—

**Table 3.** Differences of fALFF among three groups. All  $P < 0.05$ , with Alphasim corrected. MNI = Montreal Neurological Institute; L = left; R = right; Mid = middle; Inf = inferior; Sup = superior; Orb = orbital.

between neuropsychological test scores, venous blood ammonia level and gray matter volume, or fALFF values in other regions which showed the statistical differences (all  $P > 0.05$ ).

## Discussion

In the present study, we found widespread gray matter volume changes and abnormal fALFF signals, which were much more severe in diabetic cirrhosis patients. Moreover, we also found that the blood glucose levels were correlated with brain gray matter volume and spontaneous neuronal activity changes in cirrhotic patients.

Our findings show that liver cirrhosis is associated with significantly greater global gray matter loss, especially in the basal ganglia. Guevara *et al.*<sup>21</sup> found the loss of brain tissue volume was common in liver cirrhosis patients, which mainly in the frontal and parietal regions and putamen for gray matter, and their results were similar as our findings. Other studies also reported decreased gray matter volume in the globus pallidus, putamen and caudate<sup>1,3,22</sup>. Persistent abnormal metabolism changes, manifested as elevated deposition of manganese<sup>23,24</sup> may lead to permanent cell damage in the basal ganglia<sup>25,26</sup>. Another VBM study<sup>13</sup> demonstrated that the decreased gray matter volume was related to persistent exposure to hyperammonaemia, which indicated that ammonia-related cerebral edema might lead to gray matter atrophy. However, we did not find a significant correlation between venous blood ammonia level and decreased gray matter volume in our study. Difference of inclusion criteria for patient cohorts between these two studies may account for the inconsistent findings.

We found increased thalamus volume in cirrhotic patients compared with controls, which is also in line with previous findings<sup>27</sup>. According to our current knowledge, the thalamus serves as a major relay station in the brain which integrates signal input from numerous cortical regions and facilitates their communications<sup>28</sup>. One plausible interpretation is that increased thalamus volume, accompanied by decreased bilateral putamen and caudate

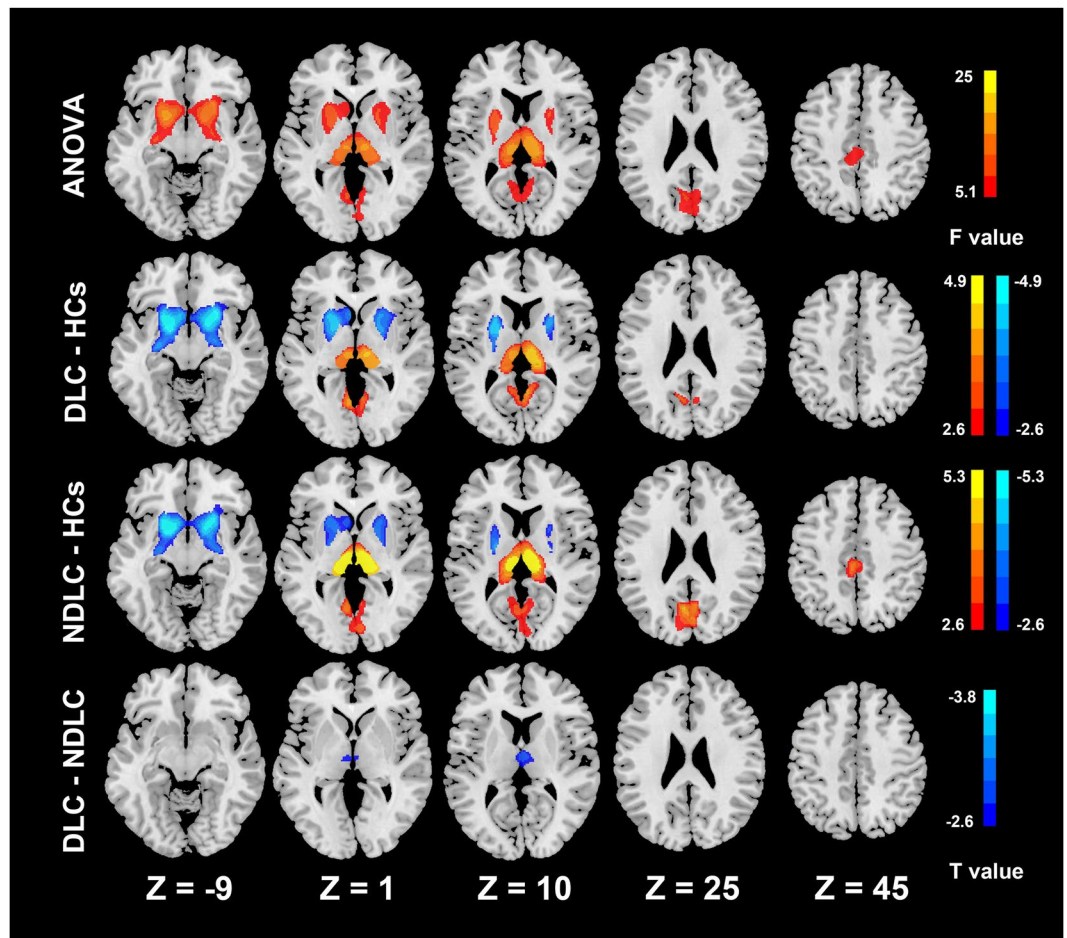


**Figure 1.** Group differences of gray matter volume. ANOVA analysis shows the volume of the putamen, thalamus, caudate, cuneus, calcarine, middle cingulate cortex and bilateral lingual gyri have significant differences among three groups. Compared with healthy controls, the diabetic cirrhosis patients group shows decreased volume in the caudate and putamen and increased volume in the thalamus and lingual gyrus. Non-diabetic cirrhosis patients group has decreased volume in the caudate and putamen and increased volume in the thalamus, middle cingulate cortex, cuneus and calcarines. The diabetic cirrhosis patients group has decreased volume in the thalamus compared with the non-diabetic cirrhosis patients group (all  $p < 0.05$ ). ANOVA = analysis of variance, DLC = diabetic liver cirrhosis, NDLC = non-diabetic liver cirrhosis, HCs = healthy controls.

volumes, is a reactive hypertrophy of relay nuclei within cortical-basal ganglia-thalamic circuits<sup>29,30</sup>. Another possible reason for the thalamic enlargement is the compensatory effect for the basal ganglia dysfunction, which is a common finding (symmetric basal ganglia hyperintensity in T1 weighted images) in cirrhosis patients<sup>31</sup>. Further subgroup analysis showed decreased volume of the thalamus in diabetic cirrhosis patients compared with non-diabetic cirrhosis patients. This is a very interesting finding in our study. Decreased thalamus volume in diabetic cirrhosis patients can be resulted from insulin resistance in T2DM which could reduce glucose metabolism in the brain tissues<sup>32</sup>, thus inhibiting the compensatory mechanisms of the thalamus. As a consequence, the increased thalamus volumes were decreased in diabetic cirrhosis patients compared with non-diabetic cirrhosis patients. Thalamus atrophy has been reported in type 1 diabetes in a recent meta analysis<sup>33</sup>. However, further studies with large sample size are needed to uncover this interesting finding.

Amplitude of low-frequency fluctuation (ALFF) algorithm proposed by Zang *et al.*<sup>34</sup> has been widely used in functional MR imaging studies. However, ALFF has some limitations in itself, such as sensitive to the physiological noise. Thus, Zou *et al.* proposed the fALFF algorithm to improve these shortcomings of ALFF<sup>15</sup>. The fALFF algorithm is an advanced technique which can effectively minimize the physiological related noise around the major vessels, thus providing a more specific index of low frequency oscillatory phenomena. In contrast to the traditional measurement of the ALFF, fALFF measurements are more reliable and more specific to reflect intrinsic neural activities<sup>15,35</sup>. In this study, we found that both patient groups showed the similar patterns of fALFF alterations. The main difference between two patient groups was that the diabetic cirrhosis patients showed decreased fALFF signals in the bilateral caudates when compared with non-diabetic cirrhosis patients. We speculate that the decreased fALFF in the occipital regions may underline the potential cognitive abnormalities relative to visual

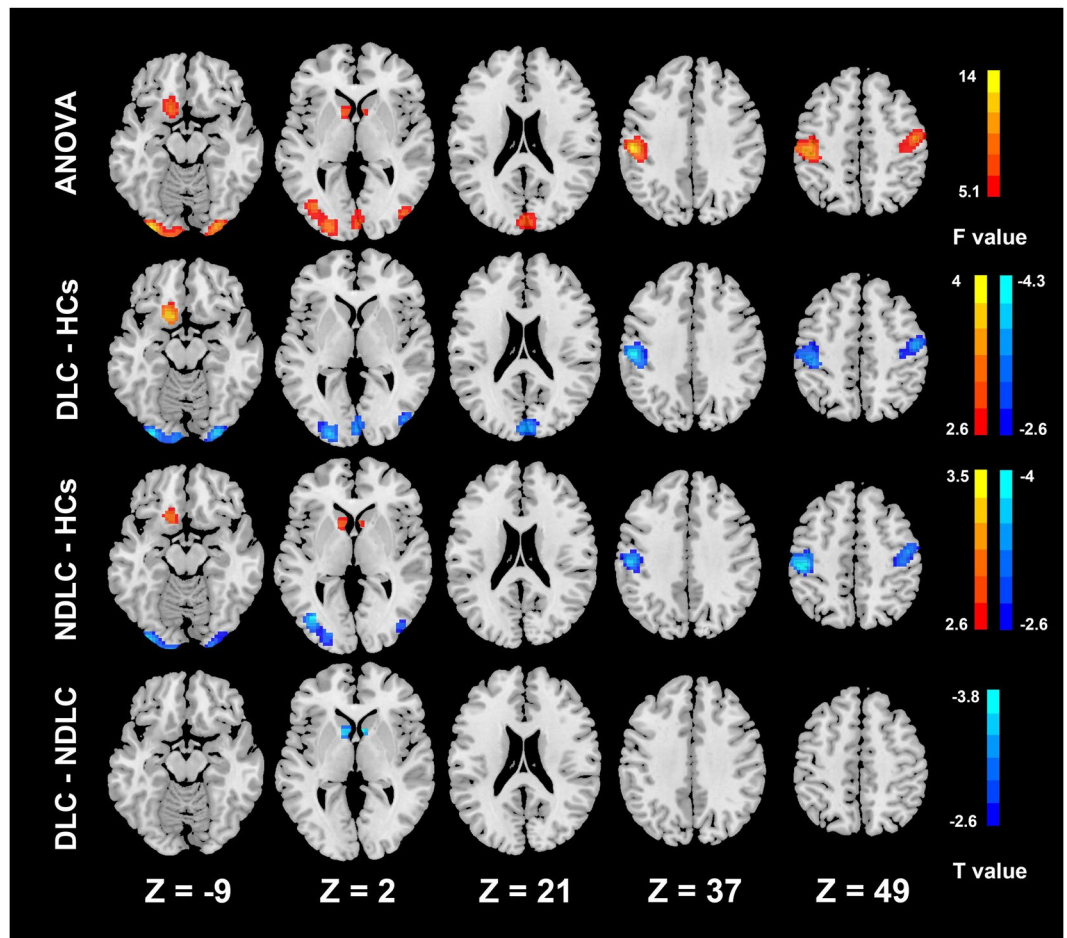


**Figure 2.** Group differences of fALFF. ANOVA analysis shows fALFF values of the caudate, occipital lobe, left postcentral gyrus, right precentral gyrus, left supramarginal gyrus and left frontal lobe have significant differences among three groups. Compared with controls, the diabetic cirrhosis patients group shows decreased fALFF values in the occipital lobe, left postcentral gyrus, right precentral gyrus and left supramarginal gyrus and increased fALFF values in the frontal lobe. Non-diabetic cirrhosis patients group has decreased fALFF values in the occipital lobe, left postcentral gyrus, right precentral gyrus and left supramarginal gyrus and increased fALFF values in the caudate and left frontal lobe. The diabetic cirrhosis patients group has decreased fALFF values in the caudate compared with the non-diabetic cirrhosis patients group (all  $p < 0.05$ ). ANOVA = analysis of variance, DLC = diabetic liver cirrhosis, NDLC = non-diabetic liver cirrhosis, HCs = healthy controls.

function which was reflected by the NCT-A and DST. And the increased fALFF signals in the frontal lobe may be a compensatory effect for the visual function decline, which represents cortical plasticity and reorganization in cirrhosis patients. However, in the comparison between the patient groups, diabetic cirrhosis patients showed decreased fALFF signals in the subcortical regions (bilateral caudates). It is possible that the basal ganglia are broadly responsible for sensorimotor coordination and the caudate nucleus is more engaged in goal-directed action<sup>36</sup>. In this study, the decreased activation in caudate nucleus may reflect the loss or decreased energy of neurons, which may be responsible for the worse performance in neuropsychological tests in diabetic cirrhosis patient group. Additionally, we found gray matter volume loss in the bilateral thalami, however, no significant fALFF changes were observed when compared with the controls in the same brain regions.

The most structural and functional changes are distributed in different brain areas in our study. However, we also found some brain areas showed both fALFF and gray matter volume changes, including the bilateral lingual gyri in the diabetic cirrhosis patients group and the bilateral caudates in the non-diabetic cirrhosis patients group. Although some studies have reported that functional connectivity coupled with structural connectivity<sup>16, 18, 19</sup>, we did not find significant correlation between the fALFF changes and gray matter volume changes in these areas. We speculate that the two methods used in our study did not reflect the connectivity changes in the brain, which may account for the different abnormal brain areas involved in the structural and functional changes.

Several limitations must be considered in our study. First, the sample size of our study is relatively small, which may limit the statistical power in the subgroup analysis. It is needed to further collect larger cohort to solve this issue in future. Second, our study was consisted of a heterogeneous patient cohort, with 4 patients having a history of hepatic encephalopathy among the cirrhotic patients. Although we strictly matched this variable, the wide

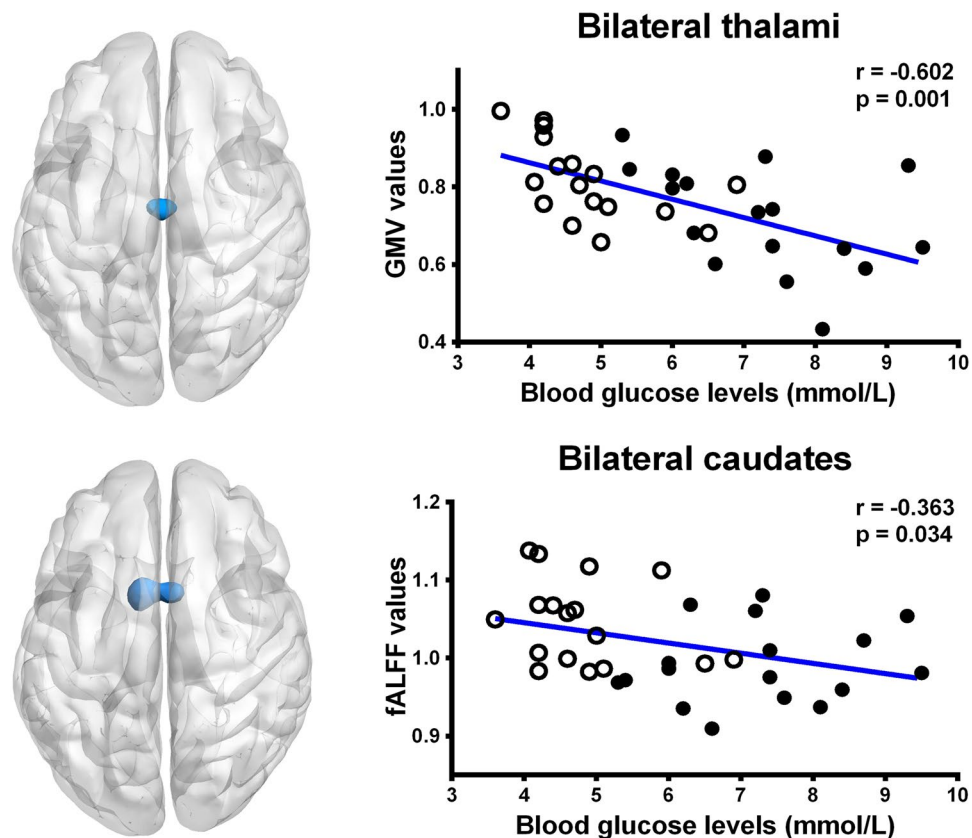


**Figure 3.** Correlation results in all cirrhosis patients. There was a negative correlation between the blood glucose levels and gray matter volume in bilateral thalami ( $r = -0.602$ ,  $P = 0.001$ ) and the fALFF values ( $r = -0.363$ ,  $P = 0.034$ ) in the bilateral caudates in all cirrhosis patients. GMV = gray matter volume; fALFF = fractional amplitude of low-frequency fluctuation; ○ = diabetic cirrhosis patient; ● = non-diabetic cirrhosis patient.

spectrum of disease state may produce the bias in our results. Third, we used only two neuropsychological tests to assess cognitive function of the patients; although they were widely used in studies regarding liver cirrhosis and recommended by the working party of 11<sup>th</sup> world congress of gastroenterology. These two tests can not detect all the cognitive impairments induced by DM and cirrhosis. Thus, more neuropsychological tests are acquired to comprehensively evaluate the cognitive status of cirrhosis patients with DM in the future. Lastly, lactulose or other medical treatments were administrated in almost all patients, which can affect brain structural and functional changes in cirrhotic patients. However, it is rather difficult to avoid these factors because the measurements have to be administrated to prevent the deterioration of diseases.

In summary, by applying both VBM and fALFF algorithms, we found brain functional and structural abnormalities were apparent and bilaterally symmetrical in cirrhotic patients, which were more widespread in cirrhosis patients with DM than those without DM. The blood glucose levels are correlated with the brain structural and functional changes in both patient groups. These findings suggest that more attention is needed in the management of DM in cirrhotic patients.

## Material and Methods

**Participants.** This is a retrospective study, which was approved by Ethics Committee of Jinling Hospital. All participants gave written informed consent before MR imaging and all methods were performed in accordance with the relevant guidelines and regulations. This study included 34 subjects with liver cirrhosis, who were subdivided into two groups according to DM history, i.e., 17 cirrhotic patients with DM, 17 cirrhotic patients without DM and 17 age, sex matched healthy controls. DM status was verified according to the following criteria: fasting plasma glucose level higher than 126 mg/dL, a non-fasting plasma glucose level higher than 200 mg/dL, or self-reported administration of anti-diabetes drugs such as insulin therapy. Each group comprised of 12 men and 5 women, who were right-handed. We also strictly matched the prevalence of overt hepatic encephalopathy and Child-Pugh scale in the two patient groups to avoid the effect of these factors on the results of cognitive assessment (Table 1). Cirrhosis was diagnosed by liver biopsy or based on the presence of biochemical, ultrasonographic, CT or MR imaging or endoscopic features of portal hypertension and/or liver dysfunction. Diabetes status was defined by subject self-report during a standardized interview (All 17 diabetic patients had T2DM). The inclusion criteria were as follows: subjects who were 18 years or older, they could finish MR examination without any MR imaging contraindications. Exclusion criteria included: (1) any drug abuse history; (2) head

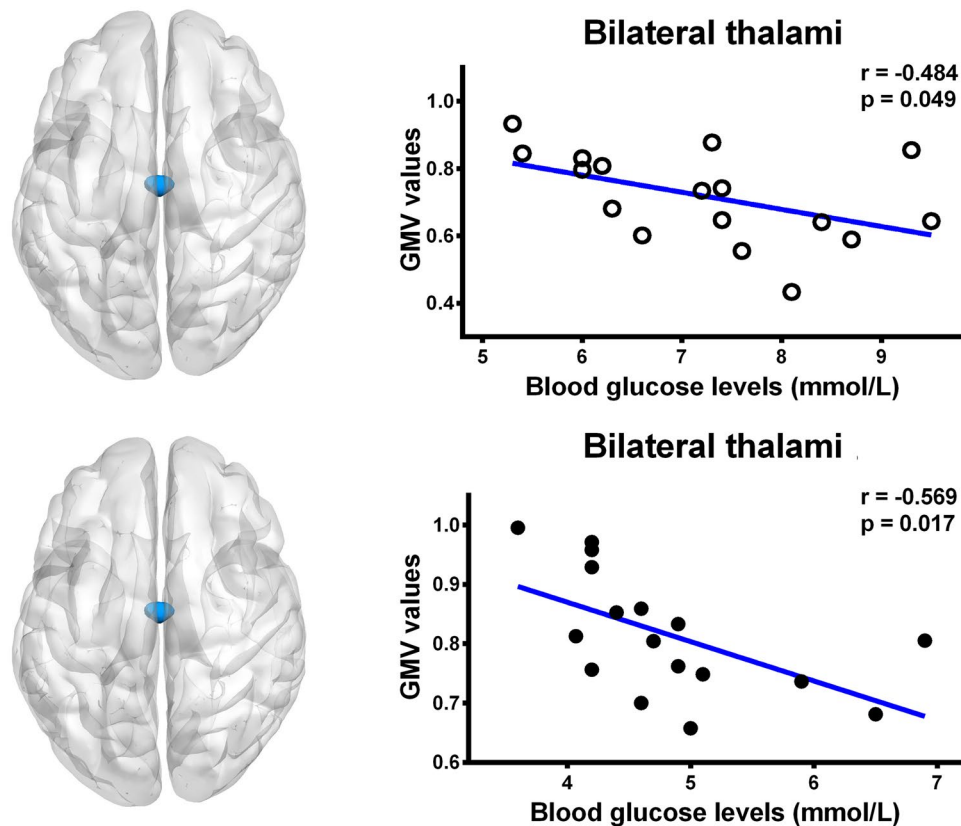


**Figure 4.** Correlation results in diabetic cirrhosis patients and non-diabetic cirrhosis patients. There was a negative correlation between the blood glucose levels and gray matter volume in bilateral thalami in diabetic cirrhosis patients group ( $r = -0.484$ ,  $P = 0.049$ ) and in non-diabetic cirrhosis patients group ( $r = -0.569$ ,  $P = 0.017$ ). GMV = gray matter volume; ○ = diabetic cirrhosis patient; ● = non-diabetic cirrhosis patient.

trauma history; (3) neurological or psychiatric disorders; (4) visual or auditory deficits; (5) rotation more than  $1.0^\circ$  or translation more than 1.0 mm during MR scanning.

**Neuropsychological Assessments.** Before MR examinations, two neuropsychological tests [number connecting test type A (NCT-A) and digit symbol test (DST)] recommended by the working party of 11<sup>th</sup> World Congress of Gastroenterology<sup>37</sup> were assessed according to the standard methods for all subjects.

**Laboratory Examinations.** Before MR scanning, blood samples of all patients were taken and blood biochemistry tests were underwent, including albumin, prothrombin time, bilirubin metabolism tests (including total bilirubin, indirect bilirubin, and direct bilirubin), glutamic oxalacetic transaminase ammonia, glutamic pyruvic transaminase, and fasting glucose levels. The severity of liver disease was determined according to Child-Pugh score. According to this scoring system, 15 patients had Child-Pugh grade A, 1 Child-Pugh grade B and 1 grade C in each patient group, respectively. All laboratory tests were unavailable for the controls.

**MR imaging data acquisition.** All MR imaging data were collected in a 3.0 Tesla scanner (TIM Trio, Siemens Medical Solutions, Erlangen, Germany), which equipped with the standard 12-channel head coil. First, high resolution T1 weighted structural images were acquired in the sagittal orientation with a magnetization prepared rapid gradient echo sequence (TR/TE = 2300 ms/2.98 ms, field of view (FOV) = 256 mm × 256 mm, flip angle =  $9^\circ$ , slice thickness = 1 mm, voxel of 1.0 mm × 1.0 mm × 1.0 mm, acquisition matrix = 256 × 256, 176 slices). A single-shot, gradient-recalled echo planar imaging sequence was used to acquire functional images (TR/TE = 2000 ms/30 ms, FOV = 240 mm × 240 mm, flip angle =  $90^\circ$ , voxel size = 3.75 mm × 3.75 mm × 4 mm, image matrix = 64 × 64, 30 axial slices) aligned along the anterior-posterior commissure to cover the whole brain. The rs-fMRI scan lasted for 500 seconds and 250 brain volumes were collected. Then, images with axial T2 fluid attenuated inversion recovery sequence (TR/TE = 9000 ms/93 ms, inversion time = 2500 ms, flip angle =  $130^\circ$ , thickness/gap = 4.0 mm/1.2 mm, matrix = 232 × 256, FOV = 220 mm × 220 mm) was conducted to exclude clinically silent lesions. The subjects were told to keep awake, relax with their eyes closed, heads still and no thinking anything else during the functional MRI scans.

**Data processing for VBM analysis.** VBM data analysis was performed using the VBM8 toolbox in the Statistical Parametric Mapping (SPM8, <http://www.fil.ion.ucl.ac.uk/spm>) software. Firstly, structural MR imaging

data were spatially normalized into standard Montreal Neurological Institute (MNI) space. Subsequently, MR images were segmented into gray and white matter and cerebrospinal fluid using the new Segment and DARTEL modules included in SPM8. Finally, the resultant images were smoothed with full width at half maximum (FWHM) Gaussian kernel of 8 mm.

**Data processing for fALFF analysis.** Image preprocessing for fALFF data was carried out using Data Processing Assistant for Resting State fMRI (DPARSF) and SPM8<sup>38</sup>. For each subject, the beginning ten volumes were discarded to ensure the subjects can adapt to scanning noise. Slice-timing and realignment were then performed in SPM8. Then, the functional images were coregistered to the individual 3D T1 weighted images. The resulting normalized functional data were spatially smoothed with FWHM Gaussian kernels of 6 mm, while linear trends of time courses were removed. Finally, all images underwent temporally filtered (0.01–0.1 Hz) to remove the effects of high-frequency noises and very low-frequency drift.

For fALFF analysis, with a fast Fourier transform, the time series of each voxel was transformed to the frequency domain. Then we calculated the sum of the frequencies in the low frequency band (0.01–0.1 Hz). We also computed the power spectrum and performed square root transform at each voxel. The averaged square root was regarded as ALFF value. For each subject, ALFF value of each voxel was normalized by the mean within-brain ALFF value. The fALFF value is the ratio between the sum of power spectrum of low-frequency (0.01–0.1 Hz) and the sum of the entire frequency range.

**Statistical Analysis.** Analysis of demographic, neuropsychological scores and clinical variables was performed with SPSS software (version 18 SPSS, IBM). Gender difference among three groups was evaluated with  $\chi^2$  test. The normality of quantitative data was analyzed with Kolmogorov-Smirnov test. Normally distributed data, expressed as mean  $\pm$  standard deviation (SD), were analyzed by using ANOVA test. The variance homogeneity of these data was examined with Bartlett test. The Fisher test was used if the variance was homogeneous, or else, Brown-Forsythe approximate variance analysis was used. Non-normal distribution data, reported as median and inter-quartile range [M (QU-QL)], were analyzed with independent sample nonparametric test. If ANOVA test showed the significant differences, we further used post hoc analysis to perform inter-group comparisons. A P value  $< 0.05$  was considered as statistical difference.

We used the dpabi software package to analyze structural and functional imaging data<sup>39</sup>. To assess the effect of comorbid DM on spontaneous neuronal activity and gray matter volume in cirrhosis patients, smoothed images were analyzed first by an ANOVA for the three groups, followed by post hoc unpaired two-sample t-tests. Sex and age were imported as nuisance covariates for all inter-group analyses. All the analysis results were regarded as statistically significant at P values  $< 0.05$  (Alphasim correction) and corrected for multiple comparisons with least significant difference (LSD). LSD is a common post hoc multiple comparison tests, which is recommended by the dpabi software (41) and applied in lots of brain MR studies<sup>40</sup>. Clinical variables and neuropsychological scores (including NCT-A and DST) were correlated with imaging parameters which showed the statistical difference in aforementioned ANOVA results in the patient groups using Pearson correlation analysis.

**Data Availability.** The datasets generated during and/or analysed during the current study are available from the corresponding author on reasonable request.

## References

1. Qi, R. *et al.* Grey and white matter abnormalities in minimal hepatic encephalopathy: a study combining voxel-based morphometry and tract-based spatial statistics. *Eur Radiol.* **23**, 3370–3378 (2013).
2. Qi, R. *et al.* Altered resting-state brain activity at functional MR imaging during the progression of hepatic encephalopathy. *Radiology.* **264**, 187–195 (2012).
3. Zhang, L. J. *et al.* The effect of hepatic encephalopathy, hepatic failure, and portosystemic shunt on brain volume of cirrhotic patients: a voxel-based morphometry study. *Plos One.* **7**, e42824 (2012).
4. Zhang, L. J., Yang, G., Yin, J., Liu, Y. & Qi, J. Neural mechanism of cognitive control impairment in patients with hepatic cirrhosis: a functional magnetic resonance imaging study. *Acta Radiol.* **48**, 577–587 (2007).
5. Garcia-Compean, D., Jaquez-Quintana, J. O., Gonzalez-Gonzalez, J. A. & Maldonado-Garza, H. Liver cirrhosis and diabetes: Risk factors, pathophysiology, clinical implications and management. *World J Gastroenterol.* **15**, 280–288 (2009).
6. Hickman, I. J. & Macdonald, G. A. Impact of diabetes on the severity of liver disease. *Am J Med.* **120**, 829–834 (2007).
7. Cheng, G., Huang, C., Deng, H. & Wang, H. Diabetes as a risk factor for dementia and mild cognitive impairment: a meta-analysis of longitudinal studies. *Intern Med J.* **42**, 484–491 (2012).
8. Mortimer, J. A. *et al.* High normal fasting blood glucose is associated with dementia in Chinese elderly. *Alzheimers Dement.* **6**, 440–447 (2010).
9. Chen, H. J., Zhang, L. J. & Lu, G. M. Multimodality MRI findings in patients with end-stage renal disease. *Biomed Res Int.* **2015**, 697402 (2015).
10. Baron, J. C. *et al.* *In vivo* mapping of gray matter loss with voxel-based morphometry in mild Alzheimer's disease. *Neuroimage.* **14**, 298–309 (2001).
11. Yamasue, H. *et al.* Voxel-Based analysis of MRI reveals anterior cingulate gray-matter volume reduction in posttraumatic stress disorder due to terrorism. *Proc Natl Acad Sci USA* **100**, 9039–9043 (2003).
12. Musen, G. *et al.* Effects of type 1 diabetes on gray matter density as measured by voxel-based morphometry. *Diabetes.* **55**, 326–333 (2006).
13. Iwasa, M. *et al.* Regional reduction in gray and white matter volume in brains of cirrhotic patients: voxel-based analysis of MRI. *Metab Brain Dis.* **27**, 551–557 (2012).
14. Biswal, B., Yetkin, F. Z., Haughton, V. M. & Hyde, J. S. Functional connectivity in the motor cortex of resting human brain using echo-planar MRI. *Magn Reson Med.* **34**, 537–541 (1995).
15. Zou, Q. H. *et al.* An improved approach to detection of amplitude of low-frequency fluctuation (ALFF) for resting-state fMRI: Fractional ALFF. *J Neurosci Methods* **172**, 137–141 (2008).
16. Greicius, M. D., Supekar, K., Menon, V. & Dougherty, R. F. Resting-State Functional Connectivity Reflects Structural Connectivity in the Default Mode Network. *Cereb Cortex.* **19**, 72–78 (2009).



17. Liao, W. *et al.* Default mode network abnormalities in mesial temporal lobe epilepsy: A study combining fMRI and DTI. *Hum Brain Mapp.* **32**, 883–895 (2011).
18. Zhang, Z. *et al.* Altered functional-structural coupling of large-scale brain networks in idiopathic generalized epilepsy. *Brain.* **134**, 2912–2928 (2011).
19. Ji, G. J. *et al.* Generalized tonic-clonic seizures: aberrant interhemispheric functional and anatomical connectivity. *Radiology.* **271**, 839–847 (2014).
20. Long, Z. *et al.* Thalamocortical dysconnectivity in paroxysmal kinesigenic dyskinesia: Combining functional magnetic resonance imaging and diffusion tensor imaging. *Mov Disord.* **32**, 592–600 (2017).
21. Guevara, M. *et al.* Cerebral magnetic resonance imaging reveals marked abnormalities of brain tissue density in patients with cirrhosis without overt hepatic encephalopathy. *J Hepatol.* **55**, 564–573 (2011).
22. Lin, W. C. *et al.* Significant volume reduction and shape abnormalities of the basal ganglia in cases of chronic liver cirrhosis. *AJNR Am J Neuroradiol.* **33**, 239–245 (2012).
23. Kulisevsky, J. *et al.* Pallidal hyperintensity on magnetic resonance imaging in cirrhotic patients: Clinical correlations. *Hepatology.* **16**, 1382–1388 (1992).
24. Pujol, A., Graus, F., Peri, J., Mercader, J. M. & Rimola, A. Hyperintensity in the globus pallidus on T1-weighted and inversion-recovery MRI: a possible marker of advanced liver disease. *Neurology.* **41**, 1526–1527 (1991).
25. Kim, Y. *et al.* Increase in signal intensities on T1-weighted magnetic resonance images in asymptomatic manganese-exposed workers. *Neurotoxicology.* **20**, 901–907 (1999).
26. Dobson, A. W., Erikson, K. M. & Aschner, M. Manganese neurotoxicity. *Ann N Y Acad Sci.* **1012**, 115–128 (2004).
27. Chen, H. J. *et al.* Structural and functional cerebral impairments in cirrhotic patients with a history of overt hepatic encephalopathy. *Eur J Radiol.* **81**, 2463–2469 (2012).
28. Herrero, M. T., Barcia, C. & Navarro, J. M. Functional anatomy of thalamus and basal ganglia. *Childs Nerv Syst.* **18**, 386–404 (2002).
29. Haber, S. N. & Calzavara, R. The cortico-basal ganglia integrative network: the role of the thalamus. *Brain Res Bull.* **78**, 69–74 (2009).
30. Steriade, M. & Llinás, R. R. The functional states of the thalamus and the associated neuronal interplay. *Physiol Rev.* **68**, 649–742 (1988).
31. Rovira, A., Alonso, J. & Córdoba, J. MR imaging findings in hepatic encephalopathy. *AJNR Am J Neuroradiol.* **29**, 1612–1621 (2008).
32. Baker, L. D. *et al.* Insulin resistance and Alzheimer-like reductions in regional cerebral glucose metabolism for cognitively normal adults with prediabetes or early type 2 diabetes. *Arch Neurol.* **68**, 51–57 (2011).
33. Moulton, C. D., Costafreda, S. G., Horton, P., Ismail, K. & Fu, C. H. Meta-analyses of structural regional cerebral effects in type 1 and type 2 diabetes. *Brain Imaging Behav.* **9**, 651–662 (2015).
34. Zang, Y. F. *et al.* Altered baseline brain activity in children with ADHD revealed by resting-state functional MRI. *Brain Dev.* **29**, 83–91 (2007).
35. Zuo, X. N. *et al.* The oscillating brain: complex and reliable. *Neuroimage.* **49**, 1432–1445 (2010).
36. Grahn, J. A., Parkinson, J. A. & Owen, A. M. The cognitive functions of the caudate nucleus. *Prog Neurobiol.* **86**, 141–155 (2008).
37. Ferenci, P. *et al.* Hepatic encephalopathy—definition, nomenclature, diagnosis, and quantification: final report of the working party at the 11th World Congresses of Gastroenterology, Vienna, 1998. *Hepatology.* **35**, 716–721 (2002).
38. Chao-Gan, Y. & Yu-Feng, Z. DPARSF: a MATLAB toolbox for “pipeline” data analysis of resting-state fMRI. *Front Syst Neurosci.* **4**, 13 (2010).
39. Yan, C. G., Wang, X. D., Zuo, X. N. & Zang, Y. F. DPABI: Data Processing & Analysis for (Resting-State) Brain Imaging. *Neuroinformatics.* **14**, 339–351 (2016).
40. Wang, D., Guo, Z. H., Liu, X. H., Li, Y. H. & Wang, H. Examination of hippocampal differences between Alzheimer disease, amnesic mild cognitive impairment and normal aging: diffusion kurtosis. *Curr Alzheimer Res.* **12**, 80–87 (2015).

## Acknowledgements

The authors gratefully acknowledge all participants for their contribution to this research, and appreciate the grants from Natural Scientific Foundation of China (81322020, 81230032 to L.J.Z.) and Program for New Century Excellent Talents in University (NCET-12-0260 to L.J.Z.).

## Author Contributions

Y.F.W. conducted the initial analyses and drafted the initial manuscript; X.K. conducted the initial analyses, and reviewed and revised the manuscript; G.M.L. and L.J.Z. conceptualized and designed the study, conducted the initial analyses, and reviewed and revised the manuscript. All authors read and contributed to the final manuscript.

## Additional Information

**Competing Interests:** The authors declare that they have no competing interests.

**Publisher's note:** Springer Nature remains neutral with regard to jurisdictional claims in published maps and institutional affiliations.



**Open Access** This article is licensed under a Creative Commons Attribution 4.0 International License, which permits use, sharing, adaptation, distribution and reproduction in any medium or format, as long as you give appropriate credit to the original author(s) and the source, provide a link to the Creative Commons license, and indicate if changes were made. The images or other third party material in this article are included in the article's Creative Commons license, unless indicated otherwise in a credit line to the material. If material is not included in the article's Creative Commons license and your intended use is not permitted by statutory regulation or exceeds the permitted use, you will need to obtain permission directly from the copyright holder. To view a copy of this license, visit <http://creativecommons.org/licenses/by/4.0/>.

© The Author(s) 2017